Shear Damping Function Measurements for Branched Polymers

DANIEL A. VEGA,* SCOTT T. MILNER

ExxonMobil Research and Engineering, Route 22 East, Annandale, New Jersey 08801

Received 5 May 2006; revised 18 June 2007; accepted 21 June 2007
DOI: 10.1002/polb.21276
Published online in Wiley InterScience (www.interscience.wiley.com).

ABSTRACT: We present results for step-strain experiments and the resulting damping functions of polyethylene blends of different structures, including solutions of linear, star and comb polymers. Remarkably, an entangled melt of combs exhibits a damping function close to that for entangled linear chains. Diluting the combs with faster-relaxing material leads to a more nearly constant damping function. We find similar behavior for blends of commercial low density polyethylene LDPE. Our results suggest a simple picture: on timescales relevant to typical damping-function experiments, the rheologically active portions of our PE combs as well as commercial LDPE are essentially chain backbones. When strongly entangled, these exhibit the Doi-Edwards damping function; when diluted, the damping function tends toward the result for unentangled chains described by the Rouse model – namely, no damping. ©2007 Wiley Periodicals, Inc. J Polym Sci Part B: Polym Phys 45: 3117–3136, 2007
Keywords: branched; rheology; star polymers

INTRODUCTION

At present, linear viscoelastic properties of model polymers with different architectures (linears, stars, combs, etc) are relatively well understood in terms of the tube model.[1] Recently, by including concepts such as reptation, arm retraction, and dynamic dilution, Milner and McLeish developed a "parameter free" theory that describes the linear relaxation properties of star polymers,[2] linear polymers,[3] and star/linear polymer blends.[4] This approach has also been applied to other structures such as pompom, H's, and comb polymers.[5–7]

On the other hand, the nonlinear viscoelastic properties of branched polymers are poorly understood. Although the step-strain behavior of entangled linear[8] and star polymers[9] are reasonably well described in terms of the Doi–Edwards model (DE),[1] the limits of applicability of the theory have not been clearly established. In addition, there are only a few experimental studies on model branched molecules other than stars, and structure–property relationships are not well established.

Given its practical importance, most studies have focused on commercial long-chain branched (LCB) polymers such as low density polyethylene (LDPE). The introduction of small amounts of LCB is an effective way to increase the melt strength of commercial polymers. The branched structure is thought to be responsible for the desirable extensional properties of LDPE. In uniaxial and biaxial extension, LDPE exhibits strain hardening.[10,11] The control of strain hardening is of high practical importance. For example, this property is thought to be responsible for the superior bubble stability of LDPE in film blowing as compared with unbranched polymers with similar molecular weights. However, since

Correspondence to: S. T. Milner (E-mail: scott.t.milner@exxonmobil.com)
**Permanent address:* Department of Physics, Universidad Nacional del Sur, Argentina.

Journal of Polymer Science: Part B: Polymer Physics, Vol. 45, 3117–3136 (2007)

the chain architecture of this commercial polymer is not known in detail, it is difficult to establish the basic mechanisms that control the nonlinear dynamics.

Experiments show that beyond some characteristic time τ_k after imposing a step shear strain of amplitude γ, the time-dependent relaxation modulus $G(t,\gamma)$ for many different polymers can be factored as:[12–14]

$$G(t,\gamma) = G(t)\, h(\gamma) \tag{1}$$

in terms of the linear relaxation modulus $G(t)$ and the strain dependent "damping function" $h(\gamma)$.[15] This feature is known as time-strain separability.[16,17]

In entangled linear polymers with moderately narrow molecular weight distribution ($M_w/M_n < 4.0$), $h(\gamma)$ is reasonably well described by the DE model. However, linear polymers with a few entanglements per chain or broad molecular weight distributions exhibits a weaker dependence on γ than predicted by DE.[16]

The DE theory describes stress in entangled linear polymers shortly after a step-strain. "Shortly after" means on timescales such that chains can relax their contour length within their tubes, that is, many Rouse times after the step-strain.

Explicitly, the DE result for the stress $\sigma(t = 0+)$ is:[1]

$$\sigma(\gamma) = \frac{kT\, c_{eq}}{\langle|\mathbf{E}\cdot\mathbf{u}|\rangle_0}\left\langle \mathbf{E}\cdot\mathbf{u}\frac{\mathbf{E}\cdot\mathbf{u}}{|\mathbf{E}\cdot\mathbf{u}|}\right\rangle_0. \tag{2}$$

Here $\mathbf{E}$ is the second-order deformation gradient, c_{eq} is the equilibrium concentration of entanglement strands, and $\langle\rangle_0$ denotes an average over an isotropic distribution function of unit vectors $\mathbf{u}$.[1] The stress then relaxes with the linear relaxation function regardless of strain amplitude, as the tube explores new conformations by curvilinear diffusion (reptation). Thus the DE damping function is $h(\gamma) = \sigma(E(\gamma))/(G_0\gamma)$, where G_0 is the rubberlike modulus of the material.

For marginally entangled polymers, one might hope to crudely describe the dynamics using the Rouse model–for which the stress after a step-strain is $\sigma(t) = \gamma\, G(t)$, so that $h(\gamma)$ is equal to unity.

The dotted lines of Figure 1 shows experimental results of nonlinear relaxation modulus $G(t,\gamma)$ for an entangled PS solution at different values of strain (experimental details presented below). The figure inset shows the reduced relaxation modulus $G(t,\gamma)/h(\gamma)$. Each curve for $\gamma \geqslant 0.5$ has been shifted vertically so it superposes onto the curve corresponding to small strain ($\gamma = 0.2$) in the long time region. Observe that the different relaxation curves superpose only at sufficiently long times. Below the characteristic time of approximately 6 s, time-strain separability fails.

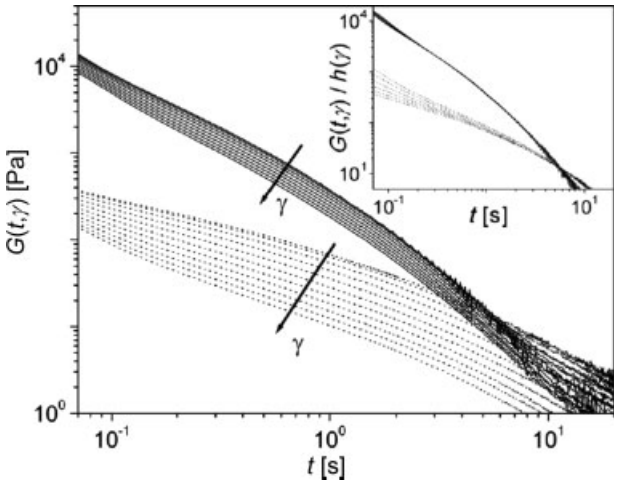

Figure 1. Non-linear relaxation modulus $G(t,\gamma)$ for samples PSL1 (solid curves) and PSL2 (dotted curves) at $T = 140$ °C and $T = 60$ °C, respectively. Shear strains increase for each sample from $\gamma = 0.2$ to $\gamma = 5.0$ in the direction indicated in the figure by an arrow [strains: 0.2 (linear), and 0.5 through 5.0 in steps of 0.5]. Inset: shifted nonlinear modulus $G(t,\gamma)/h(\gamma)$ for PSL1 and PSL2.

According to previous studies, the time characterizing the failure of the time-strain superposability τ_k is related to the time required for a complete relaxation of the contour length τ_S[1,8] through $\tau_S \sim \tau_k \sim 4.5\tau_R$, where τ_R is the longest Rouse time of the chain .

However, recent experiments of Sanchez-Reyes and Archer [17] and Inoue et al.[18] suggest that τ_k is not dictated by τ_R. Experiments with well entangled linear polystyrene solutions show that good superposition is possible only at times comparable to the terminal relaxation time of the chain τ_d ($\tau_k \sim \tau_d$). In more weakly entangled systems, τ_S and τ_k become very close each other.[17]

Figure 2 shows the comparison between the theoretical results of DE for $h(\gamma)$ and the experimental data resulting from the data collapse of Figure 1 (square symbols). Observe that the agreement between the DE model and experiments is very good.

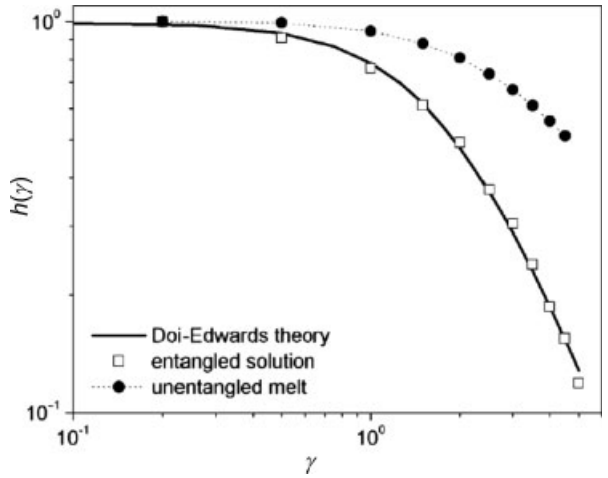

Figure 2. Long time damping function $h(\gamma)$ for linear polymers in an unentangled melt PSL1 (circles) and an entangled solution PSL2 (squares). The solid curve is the DE damping function ($h_{DE}(\gamma)$) (without independent alignment approximation).[1]

However, although the DE model gives a very good description for $h(\gamma)$ for entangled linear polymers with relatively narrow molecular weight distributions, important deviations from DE have been observed on other polymeric systems.[16]

Recently, careful experiments by Sanchez-Reyes and Archer[17] shed light on an old observation for very high molecular weight polymers of damping functions $h(\gamma)$ falling below than the DE damping function. By preventing wall-slip effects, they clearly show that the long time damping function for such polymers are consistent with the DE damping function. However, a close inspection of the data shows negative deviations in $h(\gamma)$ relative to DE of about 20–30% in the strain range $\gamma = 0.2$–2.0. At present, it is not clear if this remaining discrepancy corresponds to the real behavior of highly entangled polymers, or an experimental consequence of non-idealities, such as small remaining wall-slip effects or non-uniformly distributed strains.

The situation is more complex in the case of polydisperse linear polymers or highly branched structures. In polydisperse linear systems a weaker dependence on γ in the damping function relative to DE[16] has been observed. Although the difference can be qualitatively understood as a crossover between Rouse-like and DE behaviors, at present there is no theory describing the damping function of weakly entangled linear polymers.

Polymers containing LCB, such as LDPE, also shows $h(\gamma)$ with a weaker dependence on strain relative to DE.[13,19] However, as consequence of the wide variety of relaxation process present in the system, in this case the nonlinear polymer dynamics is certainly not well understood.

Recently, Bick and McLeish[20] (BM) and Bishko et al.[21] proposed a model to describe the nonlinear step-strain of entangled polymers of general architecture. Their picture of stress "shortly after" a step strain builds on DE, by including the effect of chain segments between branch points that are unable to relax by retracting a free end. Such segments can bear additional tension, up to the point that the average increase in length of the segment $\langle |\mathbf{E}\cdot\mathbf{u}| \rangle$ approaches the segment priority.[20] The segment "priority" is defined as the minimum number of free ends of the two subtrees created by cutting the segment.

According to BM, the DE expression eq 2 for the stress tensor can be generalized for branched structures as:[20]

$$\sigma \propto \left\langle \mathbf{E}.\mathbf{u}\frac{\mathbf{E}\cdot\mathbf{u}}{|\mathbf{E}\cdot\mathbf{u}|}\right\rangle \left[\sum_{i=1}^{i<\langle|\mathbf{E}\cdot\mathbf{u}|\rangle}\frac{\phi_i\, i^2}{\langle|\mathbf{E}\cdot\mathbf{u}|\rangle}+\sum_{i>\langle|\mathbf{E}\cdot\mathbf{u}|\rangle}\phi_i\langle|\mathbf{E}\cdot\mathbf{u}|\rangle\right], \quad (3)$$

where ϕ_i is the mass fraction of segments of priority i.

Thus, according to BM the priority distribution contains all information required to calculate the damping function, and thus to relate the nonlinear stress relaxation to the topology of the branched molecule. This would be a powerful simplification because $h(\gamma)$ would be independent of many details of the polymer architecture. Observe that eq 3 indicates a decrease in damping (increase in σ) if the content of high priority material increases.

Equation 3 and the theoretical picture behind it have not been extensively tested experimentally. In one recent work[22] the BM model has been used to interpret linear and nonlinear rheological data from low-density polyethylene (LDPE) by fitting to mixtures of theoretical "pom-pom" polymers, thus inferring the priority distribution for the LDPE.

In the present study, we investigate nonlinear step-strain relaxation dynamics of blends of both model and commercial branched polyethylenes with linear polyethylenes. We focus the

study on the effect of concentration and polymer structure on the damping function.

To make contact with prior work, in Linear Polymers of the Results we present data on the damping function of linear entangled and unentangled polystyrenes. In subsequent sections, we study the effect of polymer structure on $h(\gamma)$ for two different model branched polyethylenes [stars (Stars/Linear Blends), and combs (Comb/Linear Polymer Blends)]. In Low Density Polyethylene/Linear Blends, we show data on the nonlinear viscoelastic behavior of LDPE and review previous results.

EXPERIMENTAL

Rheology

Though polyethylene is of considerable commercial importance, it poses problems for step-strain experiments. Since polyethylene has a high plateau modulus, at high strains the transducers of most rheometers are easily overloaded. To prevent this, a common tactic is to reduce the plate diameter (typically ~10 mm);[6,23,24] however, this leads to lower sensitivity and increased error at long times.

One of the main sources of error in step-strain experiments is wall slip.[17,25] If slip occurs, the applied strain is lower than the desired strain; if this is overlooked, the measured damping function will be too small. This artifact is easy to miss.

To reveal the onset of wall slip, we use a pen to draw a vertical line on the edge of the sample, and observe its deformation. If there is no slip, the line deforms affinely, and the ends of the line move with the upper and lower plates. If there is slip, the line does not deform affinely, and the central portion of the line shears less than expected.

Mechanical measurements were performed on a Rheometrics mechanical spectrometer (RMS-800, Rheometric Scientific, Piscataway, NJ) in the cone-plate geometry (25 mm diameter, 0.1 rad cone angle). Viscoelastic properties were characterized by oscillatory shear and step-strain measurements. The temperature resolution of this rheometer is ± 1 °C.

We conducted all experiments under a continuous nitrogen purge to limit thermal degradation, which we verified by comparing linear dynamic response before and after our experiments. Depending on the signal-to-noise ratio, step-strain data shown in this work corresponds to an average of between 3 and 10 different runs. Comparative experiments were done on an ARES rheometer (also from Rheometrics) with the same cone-plate geometry. Very good agreement between the data of both rheometers was obtained in both the linear and nonlinear regime.

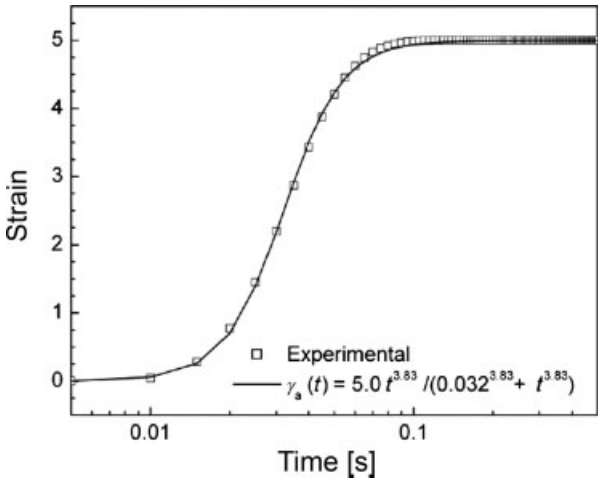

Figure 3. Measured strain in a stress relaxation experiment on the RMS-800 rheometer at $\gamma = 5.0$ (symbols). The continuous line is a phenomenological fit to the data (see text).

Step-strains are never instantaneous. Figure 3 shows the measured strain for a "step" strain experiment with a total strain of $\gamma = 5.0$ on the RMS-800 instrument. Similar results were observed with ARES. From this figure we can see that ~98% of the desired strain is achieved in a time $\tau_{step} \sim 0.08$ s.

The influence of the non-zero rise time on step-strain experiments was originally considered by Laun.[13] Whether the strain history of Figure 3 is fast enough to be considered "instantaneous" depends on the polymer relaxation spectrum. Following Laun we analyze the relaxation process using the BKZ model.[26] In step-strain experiments, the BKZ expression for the resulting stress is:

$$\sigma(t) = \int_0^\infty m(\tau)\gamma_{t,t-\tau}h(\gamma_{t,t-\tau})\mathrm{d}\tau, \qquad (4)$$

where $\sigma(t)$ is the shear stress, $m(t)$ is the memory function, and $\gamma_{t,t'}$ is the relative shear strain

between the states t and t'. Equation 4 can be rewritten as:

$$\sigma(t) = \int_0^t m(s)[\gamma(t) - \gamma(t-s)] \times h(\gamma(t) - \gamma(t-s))\mathrm{d}s + h(\gamma(t))\gamma(t)G(t) \quad (5)$$

The first term vanishes for an instantaneous step, whereupon $\sigma(t)$ approaches $h(\gamma_0)\ \gamma_0 G(t)$.

For $t \gg \tau_{\mathrm{step}}$, $\gamma(t) \simeq \gamma_0$ and the first term in eq 5 can be approximated; after some arithmetic we have:

$$\sigma(t) = \gamma_0 h(\gamma_0) G(t) + \gamma_0 m(t) Z(\gamma_0) \quad (6)$$

$$Z(\gamma_0) \equiv (1/\gamma_0)\int_0^\infty [\gamma_0 - \gamma(t')]h(\gamma_0 - \gamma(t'))\mathrm{d}t' \quad (7)$$

Here we have used the fact that $[\gamma_0 - \gamma\ (t - s)]$ is different from zero only for $t - s \lesssim \tau_{\mathrm{step}}$, which implies that $m(s) \approx m(t)$.

A"time dependent" damping function can be defined as:

$$h(\gamma, t) \equiv \frac{\sigma(t)}{\gamma_0 G(t)} \quad (8)$$

$$= h(\gamma_0) - Z(\gamma_0)\frac{\mathrm{d}}{\mathrm{d}t}\ln G(t) \quad (9)$$

(in which we have used the relation $m(t) = -\mathrm{d}G/\mathrm{d}t$). Thus the effect of a finite rise time for the step persists to some extent until the stress relaxes. However, observe that at very long times, $t > \tau_{\mathrm{d}}$, we have $d\ \ln\ G/\mathrm{d}t \approx -1/\tau_{\mathrm{d}}$. So to estimate the size of the effect of finite rise time, we need to know how big $Z(\gamma_0)$ is relative to the stress relaxation time and $h(\gamma_0)$.

Now we consider the behavior of $Z(\gamma_0)$. A change of integration variable to $\gamma = \gamma_0 - \gamma(t)$ yields

$$Z(\gamma_0) = (1/\gamma_0)\int_0^{\gamma_0} \frac{\gamma h(\gamma)\mathrm{d}\gamma}{\dot{\gamma}(\gamma)} \quad (10)$$

Making the simple approximation that during the step the shear rate is a constant $\dot{\gamma} = \gamma_0/\tau_{\mathrm{step}}$, we have

$$Z(\gamma_0) = \left(\tau_{\mathrm{step}}/\gamma_0^2\right)\int_0^{\gamma_0} \gamma h(\gamma)\mathrm{d}\gamma \quad (11)$$

Now consider two limiting cases for the shape of $h(\gamma)$: $h(\gamma) = 1$ and $h(\gamma) = 1/(1 + a^2\gamma^2)$ with $a^2 \sim 0.27$ (a simple approximation to the DE damping function). We find

$$Z(\gamma) = \tau_{\mathrm{step}}/2, \quad h(\gamma) = 1 \quad (12)$$

$$Z(\gamma) = \tau_{\mathrm{step}}\ln\left(1 + a^2{\gamma_0}^2\right)/\left(2a^2\gamma_0^2\right), \quad h(\gamma) = 1/(1 + a^2\gamma^2) \quad (13)$$

The function $\ln(1 + x^2)/x^2$ is close to unity for small x and approaches 2 ln x/x^2 for large x; thus it mimics the function $1/(1 + x^2)$ (and likewise the DE damping function), but is larger by a factor of 2 ln x where the damping function starts to fall off.

So we may say $Z(\gamma_0)$ is of order $\tau_{\mathrm{step}}h(\gamma_0)$ in both limiting cases, but larger by a factor of 2 ln γ_0 in the DE damping limit. Examining eq 9, we see that for slowly relaxing systems where the terminal relaxation time τ_{d} is much bigger than τ_{step} the corrections from finite rise time are small, and eq 1 can be employed directly to get the damping function at long times ($t \gtrsim \tau_{\mathrm{d}}$). In contrast, in quickly relaxing polymers ($\tau_{\mathrm{d}} \sim \tau_{\mathrm{step}}$) this assumption is not valid and eq 1 is not appropriate to evaluate the damping function.

One may compare $h(\gamma,t)$ to $h(\gamma_0)$ to see how big are the corrections due to finite strain rate. We calculate $h(\gamma,t)$ from the experimental data and eq 9. To calculate the stress (eq 4) we fit the measured strain history with the function $\gamma_a(t) = \gamma_0 t^n/(t_0^n + t^n)$, where γ_0 is the desired strain, and t_0 and n are fitting parameters. Figure 3 also shows the fit of the experimental data with $\gamma_a(t)$. Observe that this function describes reasonably well the applied strain.

For the systems studied in this work we found only minor differences between the long time values of $h(\gamma,t)$ and $h(\gamma_0)$, with corrections of only a few percent. In Linear Polymers of the Results, we discuss in more detail the effect of the non-zero rise time.

Materials and Methods

In this work we focus mainly on polyethylene blends of different structures. Table 1 shows the characteristics of the polyethylenes used in this work (linear, stars, combs, and LDPE).

The model branched polyethylenes were synthesized by Hadjichristidis and coworkers using techniques of anionic synthesis of polybutadiene, followed by hydrogenation to saturate the poly-

Table 1. Characteristics of the Polymers and Blends Used in this Study (Molecular Weights in kg/mol and Component Fractions in wt %)

Sample	M_{back}	M_{arm}	M_{tot}	n_e^{back}	n_e^{arm}	ϕ_{PEW}	ϕ_{main}	ϕ_{LPE}
Diluents								
PEW			3.6	4.1		100		
LPE			99	101				100
PS linears								
PSL1			20	1.5			100	
PSL2			6680	23.3			10	
PE stars								
S1	94	47	141	15.2	7.6	75	25	
S2	94	47	141	38.3	19.1	50	50	
PE combs								
C1	104	5.4	173.4	42.3	2.2	50	1.25	48.75
C2	104	5.4	173.4	42.3	2.2	50	2.5	47.5
C3	104	5.4	173.4	42.3	2.2	50	5	45
C4	104	5.4	173.4	42.3	2.2	50	10	40
C5	104	5.4	173.4	42.3	2.2	50	20	30
LDPEs								
LDPE1			239			0	100	
LDPE2			239			25	75	
LDPE3			239			50	50	
LDPE4			239			75	25	

n_e^{back} and n_e^{arm} are number of entanglements in backbone and arm, accounting for dilution effect of PEW. ϕ_{main} refers to "main" component (i.e., not PEW or LPE).

mer. The resulting polymers are model polyethylenes with well-controlled architecture. They contain a few percent butene comonomer, which results from the infrequent 1,2 insertion of butadiene in the original polymerizations, and which make essentially no difference to the rheological behavior of the polymers. Details about the synthesis of the model polyethylenes can be found in Hadjichristidis et al.[27]

In step-strain experiments, we find wall slip for well entangled linear polyethylene melts at relatively small values of strain ($\gamma \gtrsim 2.0$). Roughly speaking, we expect to encounter slip when the wall stress exceeds some threshold that the surface bond between polyethylene and the plate can support. Then, the onset of wall slip will depend on surface characteristics and the dynamic modulus on the timescale at which the step is imposed.

In our experiments, the maximum shear rates applied during the imposition of the step strain were $\dot{\gamma}_{max} \lesssim 100\ s^{-1}$. We observe the onset of slip in polymers with a high frequency storage modulus (at $\omega = 100$ rad/s) bigger than about 2×10^5 Pa.

Sanchez-Reyes and Archer[17] showed that slip can be dramatically reduced by attaching a single layer of micron-sized glass beads to the shear surfaces. By this method, they found a roughly universal damping function for entangled linear polystyrenes, irrespective of the number of entanglements.

In our case, instead of treating the shear surfaces, we reduce the wall stress by diluting the polymer with a low molecular weight linear polyethylene. For our branched polyethylene samples, we dilute with a low molecular weight linear polyethylene Bareco-4000 (PE wax, or PEW) at a concentration of 50 wt %.

However, although by dilution both transducer overload and wall slip can be prevented, this also speeds up the polymer dynamics at low polymer concentrations. To mitigate this effect, in samples with low branched polymer concentrations we also add to the blend an anionically synthesized entangled linear polyethylene (LPE). This allow us to adjust the properties of our branched polymer samples to made them more amenable to step-strain experiments.

Table 1 shows the characteristics of polymer blends used in this study. The parent materials for the model PE blends are: Bareco-4000 PE wax (PEW); linear PE (LPE) of about 100 kg/mol; a three-arm PE star with arm molecular

weight 47 kg/mol; and a PE comb with backbone molecular weight 104 kg/mol, arm molecular weight 5400 g/mol, and an average of 14.8 arms per comb. The LPE, stars, and combs were all made by anionic synthesis of polybutadiene followed by hydrogenation.

In Table 1, for convenience the number of entanglements n_e for the backbone (n_e^{back}) and arms (n_e^{arm}) are reported. In computing these values, we include the effect of dilution, considering only the PEW as diluent. The scaling of n_e with volume fraction is taken to be $n_e(\phi) = n_e(0)\,\phi^{4/3}$.[28] The melt value of the entanglement molecular weight for the model PE materials is taken to be 975 g/mol,[29] following the convention of Doi and Edwards[1] that defines the entanglement molecular weight in terms of the plateau modulus as $G_N^0 = (4/5)\rho kTN_A/M_e$. (The corresponding value for PS is 13.3 kg/mol.)

The polyethylene blends were made by dissolving the desired amounts of the components in boiling xylene and precipitating with an excess of cold methanol. Blends were placed under flowing nitrogen at room temperature to remove most of the solvents. When the specimen weight indicated than less than 5 wt % remained, the blends were put under vacuum to completely drive off the solvents. The blends were stabilized by the addition of 0.1 wt % antioxidant (50/50 Irganox 1076/Irgafox 168, both from Ciba Geigy).

To make contact with well-established literature data on damping functions, we also studied a linear low molecular weight polystyrene (PS) and a 10 wt % solution of high molecular weight linear PS (Polymer Source) in dibutylphthalate (Aldrich). Table 1 shows the molecular characteristics of the two linear polystyrenes used in this work, indicated in the table as PSL1 and PSL2.

Polyethylene blends and the low molecular weight PS PSL1 samples were compression molded at 160 °C. For the polystyrene solution PSL2 a sufficiently large specimen to fill the test gap was placed on the lower plate of the rheometer, and then the rheometer oven was set to a temperature just high enough to relax the normal force as the upper plate was lowered (but not so high that the material flowed of the plate before setting the gap).

To minimize strain-history effects, a minimum waiting time of about 10 terminal relaxation times was employed between repeated step-strain experiments.

RESULTS

Linear Polymers

Here we analyze the nonlinear viscoelastic behavior of an unentangled linear PS melt and an entangled PS solution.

Figure 1 shows the result of stress relaxation experiments at different values of strain for both PS systems and the inset of this figure the result of data collapse onto the linear shear relaxation modulus $G(t,\gamma = 0.2)$. Observe the good time-strain separability (TSS) at long times. Not also that the unentangled polymer PSL1 presents a weaker dependence on strain, and shows good superposition over a wider time window.

It is sometimes difficult to determine the onset of time-strain superposition, because the overlap of the different curves do not clearly define a single characteristic time. In such cases we use the procedure of Sanchez-Reyes and Archer,[17] which define the onset of superposition as the time at which $h(\gamma,t)$ becomes flat or presents a minimum. This allow us to estimate the onset of TSS at times $t \lesssim 0.2$ s for PSL1 and $t \lesssim 6.0$ s for PSL2.

Figure 4 shows the dynamic shear moduli $G'(\omega)$ and $G''(\omega)$ and dynamic viscosity $\eta^*(\omega)$ for polymers PSL1 and PSL2. In Figure 5 we show the predictions of eq 4 for both samples at two different strains. The prediction uses the fit to the finite rise-time step strain $\gamma_a(t)$, the long-

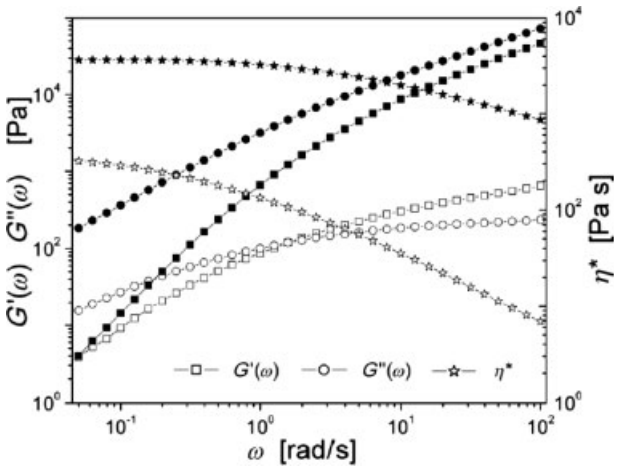

Figure 4. Dynamic storage modulus $G'(\omega)$ and loss modulus $G''(\omega)$, and dynamic viscosity $\eta^*(\omega)$ for PSL1 (filled symbols) and PSL2 (open symbols) at $T = 140$ °C and $T = 60$ °C, respectively. [Squares: $G'(\omega)$. Circles: $G''(\omega)$. Stars: $\eta^*(\omega)$].

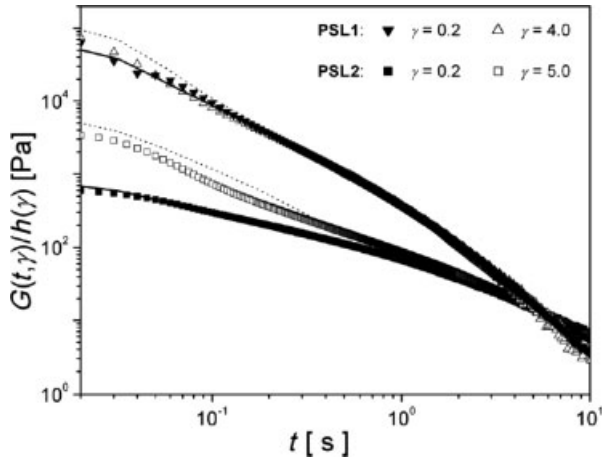

Figure 5. Reduced relaxation modulus $G(t,\gamma)/h(\gamma)$ versus time for PSL1 and PSL2 at low ($\gamma = 0.2$) and high ($\gamma = 0.4$ for PSL1, $\gamma = 0.5$ for PSL2) strains. Curves are predictions using eq 4 for low (solid curves) and high (dotted curves) strains.

time damping function $h(\gamma_0)$, and the relaxation spectrum. The relaxation spectrum is determined through a fit with the Maxwell model to the complex shear modulus $G^*(\omega)$:

$$G^*(\omega) = G'(\omega) + iG''(\omega) = \sum_i g_i \left[\frac{\omega\tau_i}{1+\omega^2\tau_i^2} + \frac{i\omega^2\tau_i^2}{1+\omega^2\tau_i^2} \right], \quad (14)$$

Here τ_i and g_i are both fitting parameters. The number of Maxwell modes is increased until the decrease in the residual error does not justify in a statistical sense any additional fitting parameters (i.e., until we are "fitting the noise"). The fit to the experimental data was made with the fitting package provided with the software Orchestrator from Rheometric Scientific.

Note in Figure 5 that the predictions of eq 4 (lines) shows a behavior very similar to the experimental data, that is, similar characteristic time for the failure of TSS and similar degree of splitting at short times of the curves corresponding to different strains. Within the BKZ model, this behavior is due entirely to the finite rise time of the step strain; if the step is instantaneous, the BKZ model predicts time-strain separability over the entire time range.

Therefore, although the failure of TSS can be produced by the presence of different mechanisms dictating the existence of a "time-dependent damping function" [e.g., $h(\gamma,t)$ going from $h(\gamma) = 1$ (Rouse) at short times towards $h(\gamma) = h_{DE}(\gamma)$ at long times], the finite rise time of the step strain appears to be sufficient to explain the failure of TSS in our experiments. Since the rise time for step strains on available commercial rheometers are of similar magnitudes, this may be a common cause of apparent failure of TSS in other data as well.

The failure of the superposition at short times is often attributed to the Rouse-like dynamics of the contour length at times lower than approximately ~5–20 -times the longest Rouse time τ_R of the chain.[1,8,9,14,18] Other have recently claimed that good superposition is possible only at times $\tau_k \sim \tau_d > \tau_R$.[17] In addition, experiments indicates a stronger dependence of τ_k on polymer concentration ($\tau_k \sim \phi^{3.2}$) when compared with a pure Rouse-like relaxation mechanism ($\tau_k \sim \phi^0$).[17]

Although different mechanisms have been proposed to explain the difference between τ_k and τ_R, it appears that the effect of the finite rise time in the step-strain experiment has been often overlooked since the work of Laun. Equation 9 makes clear that the log derivative d ln $G(t)/dt$ of stress relaxation function $G(t)$ controls the rate at which the sample "forgets" the finite rise time effect. Depending on the shape of $G(t)$, the effects of the step rise time may persist out to times of over τ_d itself.

Figure 5 shows directly that eq 4 does a reasonable job of accounting for the onset of TSS in samples PSL1 and PSL2. Now we set about estimating τ_d for the PS samples, to see if the values we obtain are consistent with the onset of TSS we observe.

To account for effects of the broad of the spectrum of relaxation times obtained from eq 14, we consider the average relaxation time proposed by Watanabe et al.,[30] which can be shown to be the product of the zero-shear viscosity and the steady-state compliance:

$$\eta_0 J_s^0 = \sum_i \tau_i^2 g_i / \sum_i \tau_i g_i \quad (15)$$

For sample PSL2 we obtained $\eta_0 J_s^0 \sim 7.5$ s, a value very close to τ_k from Figure 3. The same analysis for sample PSL1 produces for the crude estimate $\tau_d \sim 0.02$ s, which is about 10 times lower than τ_k (from Figure 1, $\tau_k \sim 0.2$ s). Using the Watanabe estimate we obtained $\eta_0 J_s^0 \sim 0.4$ s, which is likewise close to τ_k.

Figure 2 shows the long time damping function $h(\gamma)$ obtained through the shift factors employed in Figure 1, when compared with the

DE result (solid curve). The dotted line is a guide to the eye.

For linear polymer solutions the number of entanglements per chain n_e can be estimated as $n_e(\phi) = n_e^{melt}\ \phi^{4/3}$ where n_e^{melt} is the melt value.[28] From Table 1, for PSL2 we have $n_e \approx 23$, which is a well entangled sample. For this sample, in Figure 2 we observe a very good agreement of our data with DE (solid line). By reducing the number of entanglements per chain into the unentangled regime we observe a consistent decrease in the damping.

Figure 2 also shows $h(\gamma)$ for the relatively unentangled polystyrene melt PSL1 ($M_n = 2 \times 10^4$ g/mol, $n_e \approx 1.5$, at $T = 140$ °C). For this sample we observe a much weaker dependence of $h(\gamma)$ on γ. Similar behavior has been reported for other systems.[16] The decrease in damping for relatively unentangled polymers can be ascribed to a crossover to Rouse-like behavior. For concentrated but unentangled polymers, the dynamics is roughly described by the Rouse model, in which the stress is related to the strain as $\sigma(t) = \gamma G(t)$. Thus for such samples we may expect something like $h(\gamma) = 1$.

Star/Linear Blends

Although the stress relaxation processes in star and linear polymers are quite different, according to the DE model the nonlinear behavior is completely equivalent. In step-strain experiments, at $t = 0+$ both the average arm length L_0 and chain tension F_0 are larger than their equilibrium values L_{eq} and F_{eq}, respectively. Thus for entangled stars as for entangled linear chains, the contour length should relax quickly, via Rouse motion. The equilibrium, unstretched values L_{eq} and F_{eq} are recovered after a time of order τ_R. Once this fast relaxation process is completed the tube orientation should relax through arm retraction and constraint release. Beyond τ_R, the relaxation modulus for star polymers would be expected to satisfy the time-strain separability with the same damping function as linear polymers.

There are a few experimental results supporting this prediction at intermediate entanglement densities[9,31] but a more detailed study would be welcome. The results of Osaki et al.,[31] are limited to less than five entanglements per star arm, and these authors found good agreement with the DE damping function.

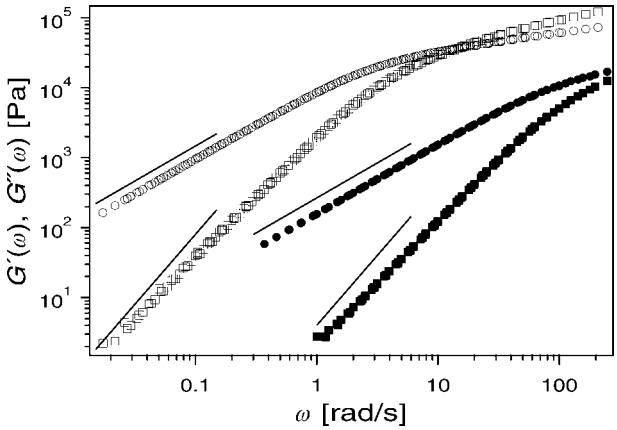

Figure 6. Dynamic moduli $G'(\omega)$ (squares) and $G''(\omega)$ (circles) for star/linear blends S1 (filled symbols) and S2 (open symbols).

On the other hand, Graessley and Vrentas[9] explored two four-arm polybutadiene star systems with many more entanglements per arm, and found some results for the damping function in disagreement with the DE model. The DE model gives a good description of the results for a star solution in Flexon 391 with about 18 entanglements per star arm. However, a star melt with about 30 entanglements per star arm shows a stronger strain dependence than DE, similarly to those observed for well entangled linear polymers.[16] In view of the new data of Sanchez-Reyes and Archer[17] for linear polymers, we are tempted to assume that wall-slip effects were present on the experiments with well entangled star polymer systems.

Here we test two star/linear blends to study the effect of dilution on the damping function. Figure 6 shows the linear dynamic rheology, and Figure 7 shows the relaxation modulus, for the star/linear blends S1 and S2. As consequence of dilution, the dynamics of the sample S1 are much faster than S2. The inset of Figure 7 shows the results of data collapse for these two polymer samples onto the corresponding linear relaxation modulus. One can obtain a reasonably good superposition for sample S1 (despite the noisy data) for times larger than approximately 0.2 s, whereas for sample S2 good superposition is possible only beyond 4 s.

As for the linear chains discussed in the previous section, we estimated the time at which one might expect time-strain superposition to be valid, by computing the average relaxation time from the linear viscoelastic spectrum using eq 15 and the data of Figure 6. We find $\eta_0 J_s^0$

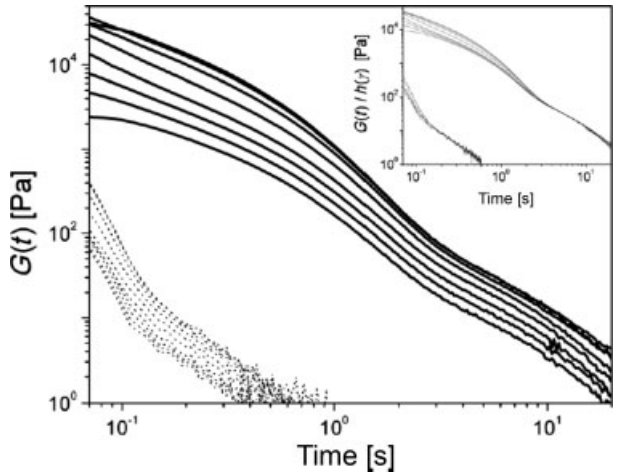

Figure 7. Relaxation modulus $G(t,\gamma)$ for star/linear blends S1 (dotted curves) and S2 (solid curves). Figure inset: shifted relaxation modulus $G(t,\gamma)/h(\gamma)$ for samples S1 and S2.

≈ 0.03 s and $\eta_0 J_s^0 \approx 0.8$ s for blends S1 and S2, respectively. These values are reasonably close to but still underestimate the the onset of TSS as evident in the inset to Figure 7.

Figure 8 shows the damping function for both star/linear blends. Observe that sample S1 presents a relatively weak dependence on strain, an expected result considering that as consequence of dilution, the arms are relatively unentangled (see Table 1).

For sample S2 the damping function presents some puzzling features. Figure 8 shows $h(\gamma,t)$ at two different times for this sample. At short times, the damping function for S2 is smaller at large strains than the DE damping function. This behavior is presumably again due to rise time effects. At long times, $h(\gamma)$ for S2 is higher than DE and becomes close to $h_{DE}(\gamma)$ at the highest values of gamma studied here for this polymer (transducer overload restricts the strain to $\gamma \lesssim 3.5$).

In Figure 7 it is evident that there is a weak, slow relaxation process in sample S2, with a characteristic time of about 5 s. This timescale well in excess of the estimated terminal time of 0.8 s using eq 15, which itself is in good agreement with a visual assessment of the approach to terminal behavior evident in Figure 6 (e.g., the location of the crossing of $G''(\omega)$ and $G''(\omega)$).

Only on further inspection in Figure 6 do we see that at low frequencies (below $\omega = 0.1$ rad/s, say) there is a weak elastic response evident, with an amplitude of perhaps 30 Pa, consistent with the long-time process evident in Figure 7. Such a process is barely evident in the corresponding data for the more dilute sample S1.

The existence of this weak, slow relaxation process in these star samples complicates the extraction of the damping function. The origin of this relaxation in these samples is not clear. Conceivably there could be some small contaminating admixture of more slowly-relaxing material, despite the care taken to synthesize the samples. Or, there could be some relaxation process generic to entangled star melts heretofore unremarked upon. In any case, present theories of stress relaxation in star melts and solutions would not account for this process.[2]

Comb/Linear Polymer Blends

Linear Viscoelastic Properties

Here, we report results on the viscoelastic properties of comb/linear blends at different concentrations. Recall that our samples C1–C5 are 50% by weight PE wax, with the remainder made up of varying amounts of PE comb and linear PE, so that as we increase the comb concentration we are doing so at the expense of the linear PE component.

Figures 9 and 10 show the storage and loss modulus for the comb/linear blends at different comb concentrations. For comparison, data on a sample without combs was included. Observe the systematic increase at low frequencies of both $G''(\omega)$ and $G'(\omega)$ as the comb content increases. Note also that in the high frequencies

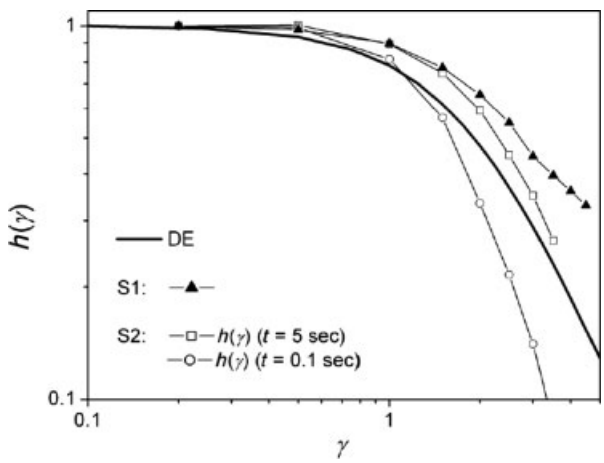

Figure 8. Damping function $h(\gamma)$ for star/linear blends S1 and S2. The solid curve is the DE damping function (without IA approximation).

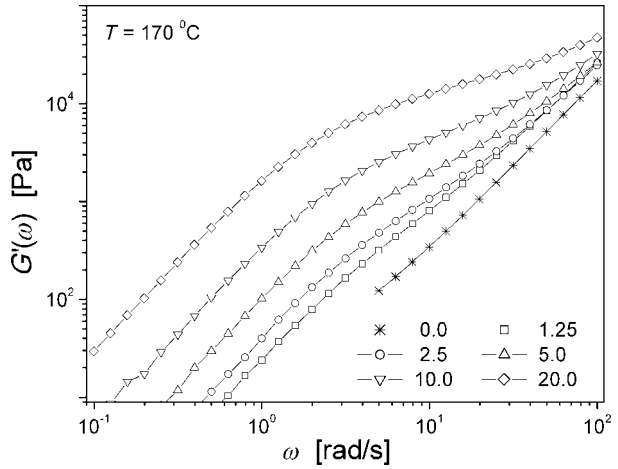

Figure 9. Dynamic storage modulus $G'(\omega)$ for comb/linear blends at $T = 170$ °C.

region (~100 rad s^{-1}) the dynamic moduli are more or less independent of comb concentration.

Figure 11 shows the dynamic viscosity $\eta^*(\omega)$ for different comb concentrations. Like the dynamic moduli, η^* (ω) becomes insensitive to comb concentration at high frequencies, while the zero shear viscosity η_0 increase strongly with ϕ_{comb}. The inset shows that the η_0 depends exponentially with the comb concentration:

$$\eta_0 \sim 706 \exp[10.3\, \phi_{comb}] \quad [\text{Pa s}] \qquad (16)$$

This star-like strong dependence reflects the concentration dependence of the effective number of entanglements per comb arm.

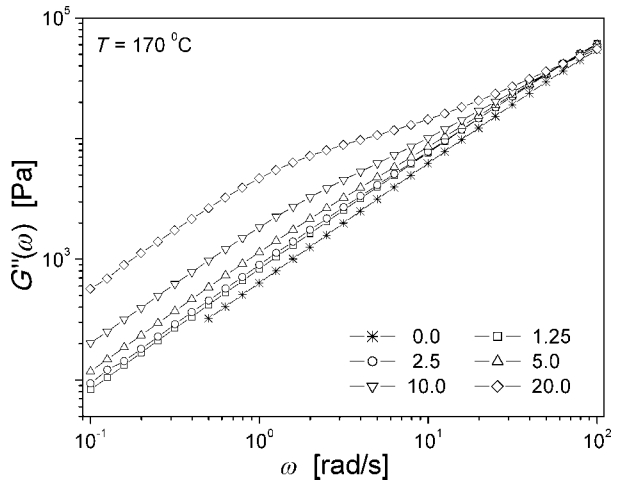

Figure 10. Dynamic loss modulus $G''(\omega)$ for comb/linear blends at $T = 170$ °C.

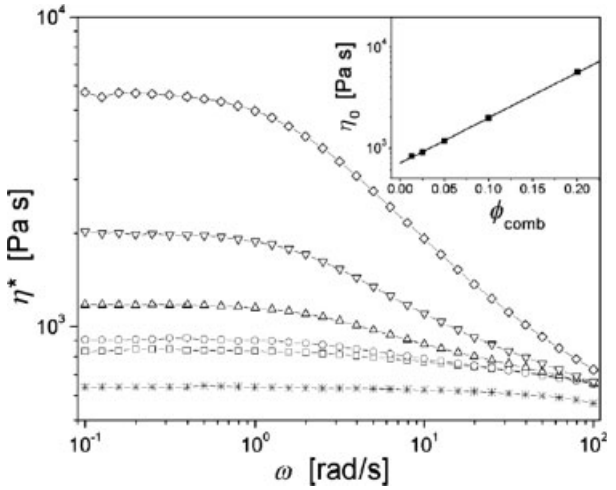

Figure 11. Dynamic viscosity $\eta^*(\omega)$ for comb/linear blends at $T = 170$ °C. Inset: zero-shear viscosity η_0 versus comb concentration (symbols) with exponential fit (line).

Step-Strain Experiments

Figure 12 shows the results of stress relaxation experiments for the comb/linear blends C1 and C5, containing 1.25 and 20 wt % combs, respectively. Evidently the relaxation spectrum broadens and the terminal times increase as the comb content increases. Figure 13 shows the data collapse of the relaxation modulus for different comb concentrations, after shifting the relaxation modulus $G(t, \gamma)$ onto the linear relaxation modulus $G(t)$. The data were superposed at long times (except that we ignore the noisy data at

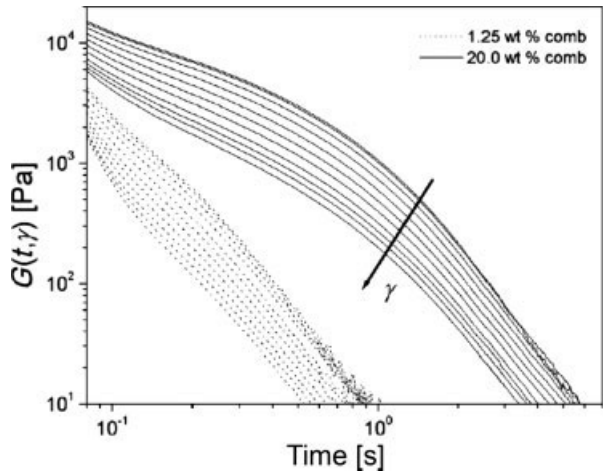

Figure 12. Nonlinear relaxation modulus $G(t,\gamma)$ for comb/linear blends C1 and C5 at strains increasing from $\gamma = 0.2$ to $\gamma = 5.0$ in the direction indicated by the arrow.

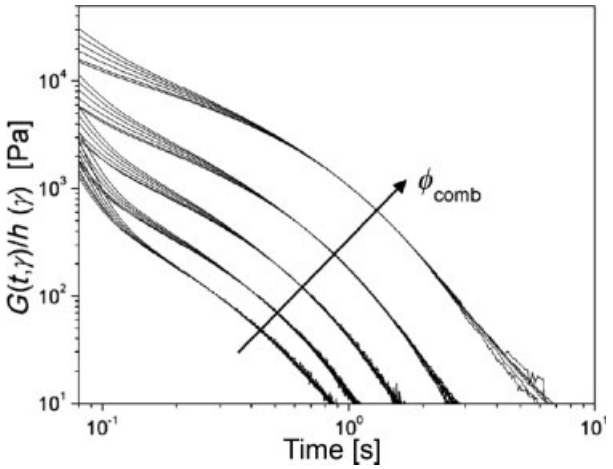

Figure 13. Reduced relaxation modulus $G(t,\gamma)/h(\gamma)$ for comb/linear blends C1–C5. Comb concentration increases in the direction indicated by an arrow from 1.25 wt % (sample C1) to 20.0 wt % (sample C5).

very late times with $G(t, \gamma) < 100$ Pa). The magnitude of the relaxation modulus grows as the comb concentration increases. Also, the onset of time-strain factorability moves to progressively longer times as the comb content increases.

Remarkably, these results on comb-linear blends are in qualitative agreement with the results of Sanchez-Reyes and Archer[17] on linear PS solutions. Their results predicts that the characteristic time τ_k scales with polymer concentration as $\tau_k \sim \phi^{3.2}$. Note that a Rouselike behavior for τ_k predicts $\tau_k \sim \phi^0$. This led Sanchez-Reyes and Archer to state that "the true separability time, evaluated from approximate overlap of $G(t, \gamma)\ h(\gamma)^{-1}$ data, appears to have very little to do with the longest Rouse relaxation time".

However, this observation is also consistent with the effects of non-zero rise time on step-strain experiments. By increasing comb concentration, the terminal relaxation time also increases. Then, according to eq 9 superposability starts at later times.

Figure 14 shows the damping function corresponding to data showed in Figure 13. We can observe that h(γ) shows a progressively weaker dependence on strain as the comb content decreases. In contrast, a theory such as that leading to eq 3 would predict the opposite trend: namely, that by decreasing the content of high priority material (in our case, decreasing comb content), the damping function should evolve towards a DE behavior.

To understand this unexpected behavior of our data, we must estimate the characteristic relaxation times of the different components of the polymer blend.

Pearson et al.[32] studied the linear viscoelastic behavior of model anionically prepared linear polyethylenes with molecular weights ranging from 10^3 to about 10^5 g/mol. His sample 3 had a molecular weight of 4.02 kg/mol, very close to our PEW, and a zero-shear viscosity of 0.7 Pa s at 175 °C. Using the plateau modulus of the model PE from Fetters[29] of $G_N = 2.28$ MPa, we make the simple estimate of a terminal relaxation time τ_{PEW} as η_0/G_N, which is about 3×10^{-7} s. Thus, although PEW is weakly entangled (about four entanglements per chain), in the timescale of the imposition of the step-strain is utterly relaxed and acts like a solvent. Since our blends contain 50 wt % of PEW, the entanglements of LPE and combs are diluted[28] by a fraction $\phi^{4/3} \approx 0.4$.

In the presence of PEW, the terminal relaxation time of LPE is reduced as consequence of dilution. The terminal relaxation time of LPE can be estimated from our data for the sample without combs as $\tau_d \sim \eta_0/G_0(\phi)$. The zero-shear viscosity for this sample is $\eta_0 \approx 640$ Pa s (Fig. 11) and the plateau modulus at a 50 wt % dilution can be estimated as $G_0(\phi) = G_0\phi^{7/3} \sim 5 \times 10^5$ Pa. Then, the terminal relaxation time $\tau_{LPE}(\phi_{PEW} = 0.5)$ for diluted LPE is roughly 10^{-3} s. Therefore, the LPE component as well relaxes quickly

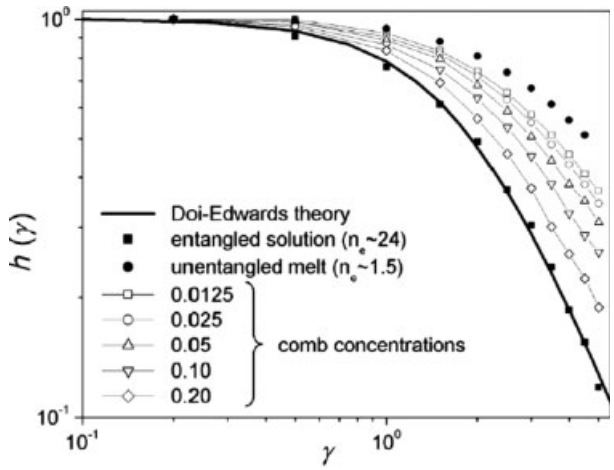

Figure 14. Damping function $h(\gamma)$ for comb/linear blends C1–C5, and unentangled linear solution PSL1 (filled circles) and entangled melt PSL2 (filled squares). The solid curve is the DE damping function.

on the timescale of the "instantaneous" step strain.

We now make a very rough estimate of the characteristic relaxation time of the comb arms, using experimental data on model PE (hydrogenated 1,4-polybutadiene) stars.

Graessley and Raju[33] have studied the rheological properties of melts and blends of low molecular weight linear and star hydrogenated polybutadienes. The data of zero-shear viscosity of four arm star melts at 190 °C from this work can be reasonably well described by:

$$\eta_0 \sim 5.4 \times 10^{-14} (M_a)^{3.6} \exp[M_a/5840] \quad [\text{Pa s}] \quad (17)$$

where M_a is the arm molecular weight.

This expression holds for polymer solutions satisfying $6.8 \times 10^3 \lesssim M_a \lesssim 3.3 \times 10^4$ g/mol. [To determine zero-shear viscosity at 170 °C (our measurement temperature) from data at $T = 190$ °C, we employed the activation energies measured by Graessley and Raju for these stars, which are found to depend on arm length.] In our case, the molecular weight of the comb arms is 5400 g/mol. From eq 17, a melt of stars with arms of this molecular weight would have a zero-shear viscosity at 170 °C of about 8 Pa s.

Note that for such an arm molecular weight we are close to but below the lower bound of applicability of eq 17. This value compares reasonably well with the data of Graessley and Raju for a four-arm star melt with similar arm molecular weight at 190 °C ($M_a \simeq 6.8 \times 10^3$ g/mol, $\eta_0 \sim 13$ Pa s) and a star/linear blend with similar effective number of entanglements ($M_a \simeq 3.3 \times 10^4$, $\phi = 0.294$, $M_a\phi^{4/3} \simeq 6.8 \times 10^3$ g/mol, $\eta_0 \sim 27$ Pa s).

Our combs (see Table 1) have about 15 arms of molecular weight 5400 g/mol, and a backbone of about 104,000 g/mol. Thus the arms are about 43 percent of the comb. The entire sample is 50 wt % PEW, and we have between 1 and 20% combs in the entire sample.

With the 7/3 power law for dilution of the plateau modulus,[28] we estimate the plateau modulus of our comb-linear-wax blends (50% wax) to be $G_0(\phi = 0.5) \approx 5 \times 10^5$ Pa. Then estimating a characteristic time using $\tau \sim \eta_0/G_0$, we find that a star arm with molecular weight of 5400 g/mol diluted by 50% wax should relax in approximately $\tau_{arms} \sim 10^{-5}$ s.

This estimate is very rough, since (1) the presence of (very) slowly relaxing comb backbones and (relatively) slowly relaxing LPE presents a dilute network of "permanent" entanglements to the star arms that can considerably slow the arm relaxation;[3] and (2) the low molecular weight of the PEW speeds up the arm relaxation, similar to what happens in the Raju-Graessley experiments in the presence of diluents.

We may hope these errors compensate to some extent. In any event, the estimated relaxation time is two orders of magnitude lower than the finite rise time of the step. Thus such short comb arms as we have may be expected to be thoroughly relaxed on experimental timescales.

Thus, after a millisecond or so, most of the constituents of the blend—polywax diluent, linear chains, and comb arms—are completely relaxed, and the stress relaxation is dominated by the relaxation of comb backbones. From Figure 11, we see that samples with the highest comb content have terminal times of order one second. Then, on the timescale of practical step-strain experiments, we can consider the comb to be like a linear chain, but with a large effective friction factor at each junction point because of the slowly relaxing arms.

Under dilution with linears and comb arms, the number of entanglements per comb backbone goes from $n_e^{bb} \lesssim 10$ to $n_e^{bb} \lesssim 0.5$, for concentrations of combs ranging from 20 down to 1.25 wt %. Then, by decreasing the comb concentration, we expect that $h(\gamma)$ changes from a DE behavior at high comb content (entangled) to behavior characteristic of unentangled linear chains at low comb content (unentangled), which is what we observe.

Thus we should not be surprised that the BM model (eq 3) does not even qualitatively describe our data. Their model describes the damping function "shortly after" an "instantaneous" step strain, where "shortly after" means on timescales of order the Rouse time of linear chains and dangling arms, and "instantaneous" means fast compared to all stress relaxations except Rouse relaxation. As our timescale estimates make clear, for our comb samples these conditions are far from being met. The comb arms of our polymers would need to be much longer to be unrelaxed on the timescale of the step-strain and the subsequent measurement.

With regard to the BM model, what remains to be considered is whether its assumptions are valid for common commercial branched polymers, such as LDPE, to which one might like to

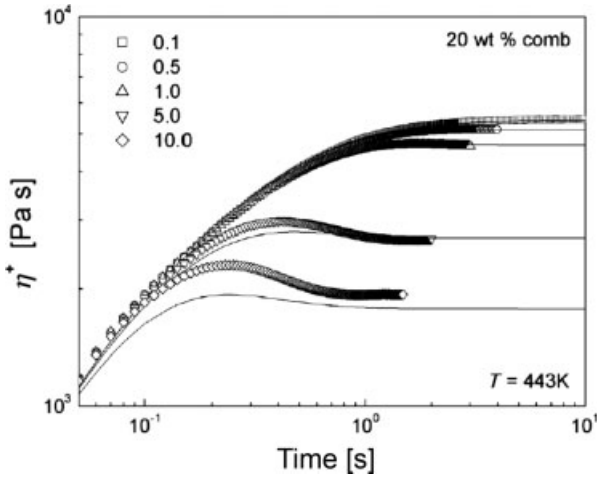

Figure 15. Transient shear data $\eta^+(t,\dot{\gamma})$ for sample C5 at $T = 170$ °C and various shear rates.

apply the model. We return to this question in Section 4 below.

Shear Start-Up Experiments

Figure 15 shows transient shear data $\eta^+(t, \dot{\gamma})$ for sample C5 ($\phi_{comb} = 0.2$) at five different shear rates, ranging from 0.1 to 10 s^{-1}. Upon increasing the shear rate the overshoot is more pronounced and the position of the maximum shifts to lower times. By plotting $\eta^+(t,\dot{\gamma})$ as function of the strain ($\gamma = \dot{\gamma}t$), it is evident that the maximum is located at approximately constant strain.

Figure 15 also includes the predictions of the BKZ model (eq 4), considering the strain history corresponding to start-up of shear rate experiments and the damping function determined via stress relaxation experiments. The BKZ model adequately predicts the behavior at low shear rates, but clearly underpredicts the size of the overshoot and also the steady-shear viscosity at the highest shear rate studied here ($\dot{\gamma} = 10$ rad/s^{-1}). This failure of BKZ is a likely result of its inaccurate handling of the stretching of the comb backbones.[34]

Recently Kasehagen and Macosko[24] have used the BKZ equation for randomly branched polybutadiene to obtain h(γ) by fitting the steady-state shear viscosity. In this work branching was produced by reacting a difunctional silane coupling agent with the vinyl groups distributed randomly along a polybutadiene precursor of molecular weight 1.4×10^5 g/mol. By employing this method, we have obtained values of $h(\gamma)$ roughly consistent with step-strain results, that is, by decreasing the comb concentration, $h(\gamma)$ presents a weaker dependence on strain. However, $h(\gamma)$ obtained through the two methods produces slightly different numerical values. The difference between $h(\gamma)$ determined by the two methods was also observed by Laun[13] for LDPE melts. Since $h(\gamma)$ determined by BKZ depends on the quality of this constitutive equation to describe the real data, in this work we use only $h(\gamma)$ determined directly from step-strain experiments.

Low Density Polyethylene/Linear Blends

In this section, we analyze the linear and nonlinear viscoelastic behavior of a commercial low density polyethylene (LDPE) melt (ExxonMobil LD 113) and blends of a LDPE with a linear low molecular weight polyethylene wax (PEW) (see Table 1 for details). The molecular weight distribution for this LDPE is showed in Figure 16.

Previous Studies on LDPE

Nonlinear rheology of LDPE of various origins has been extensively studied. Figure 17 presents damping functions from the literature for IUPAC A from Laun,[13] IUPAC X [same polymer as IUPAC A but different batch] from Samurkas et al.[11] and Dupont Alathon 20 from Soskey and Winter.[19] The weight-averaged molecular weight M_w and the polydispersity index PD = M_w/M_n for these polymers are indicated in the figure.

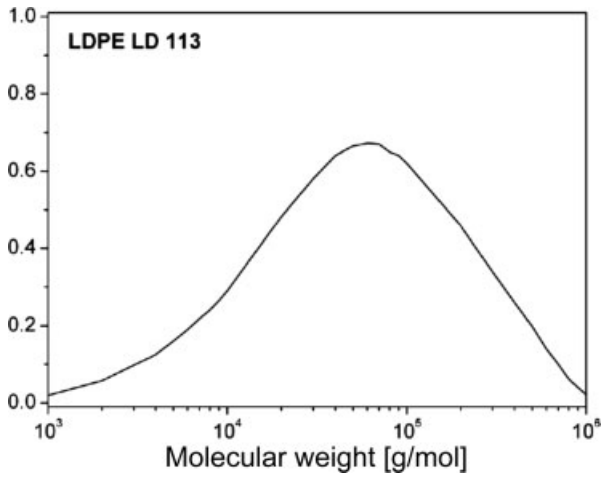

Figure 16. Molecular weight distribution for LDPE LD113 ($M_n = 4.3 \times 10^4$ g/mol, $M_w/M_n = 5.6$).

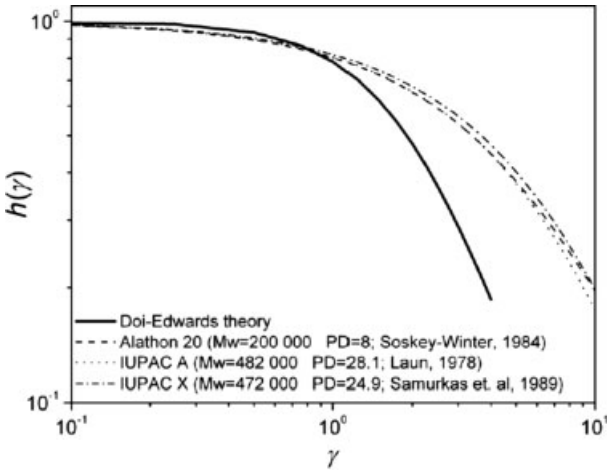

Figure 17. Literature results for damping function $h(\gamma)$ for different LDPE samples.

Observe that at high strains $h(\gamma)$ is well above DE for the three LDPEs.

Note how similar are the $h(\gamma)$ curves for all three polymers, despite the considerable difference in molecular weight distribution between the IUPAC and Alathon samples. One might have expected that such different polymers present completely different structures and hence different nonlinear responses.

Linear Viscoelastic Behavior

Figure 18 shows the shear viscosity as function of frequency for LDPE and LDPE/PEW blends at 170 °C. Observe that zero shear viscosity drops more than three orders of magnitude by reducing the LDPE concentration from 100 to 25 wt %.

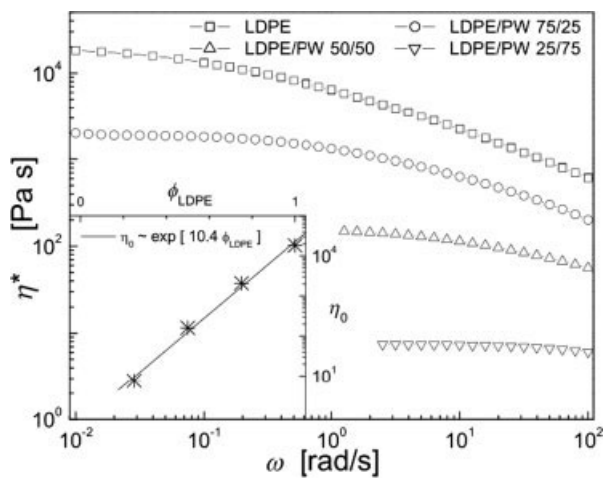

Figure 18. Shear viscosity $\eta^*(\omega)$ for LDPE and LDPE/PEW blends at T = 170°C. Inset: Zero-shear viscosity η_0 versus LDPE concentration (symbols) and exponential fit (line).

The dependence of zero-shear viscosity on LDPE concentration is displayed in the inset to Figure 18. Similar to melts and solutions of star polymers, here η_0 presents an exponential behavior on LDPE concentration: $\eta_0 \sim \exp [10.4\ \phi_{\mathrm{LDPE}}]$.

Recently, Crosby et al.[35] have analyzed the effect of dilution with squalane on different industrial polyethylenes from Dow Chemical. On a very highly branched metallocene-catalyzed polyethylene CM5 ($M_n = 7.56 \times 10^4$ g/mol, $M_w/M_n = 2.44$) these authors found an exponent very close to the value reported here ($\eta_0 \sim \exp [10.3\ \phi_{\mathrm{CM5}}]$). On the other hand, on a LDPE LD150 ($M_n = 1.04 \times 10^5$ g/mol, $M_w/M_n = 6.53$) they found a larger exponent ($\eta_0 \sim \exp[14.1\ \phi_{\mathrm{LDPE}}]$). Perhaps coincidentally, the exponent for our LDPE (10.4) and CM5 (10.3) are very close to the value obtained previously for comb/linear blends (exponent 10.3).

Stress-Relaxation Experiments

Figure 19 shows the data collapse of the relaxation modulus for different LDPE concentrations, after shifting the relaxation modulus $G(t, \gamma)$ onto the linear relaxation modulus $G(t)$.

In Figure 20 the corresponding damping functions are reported. As for the comb/linear blends, by diluting LDPE with PEW we found a systematic decrease in the damping [a more nearly constant $h(\gamma)$], although the effect is less pronounced for LDPE. This is again the opposite

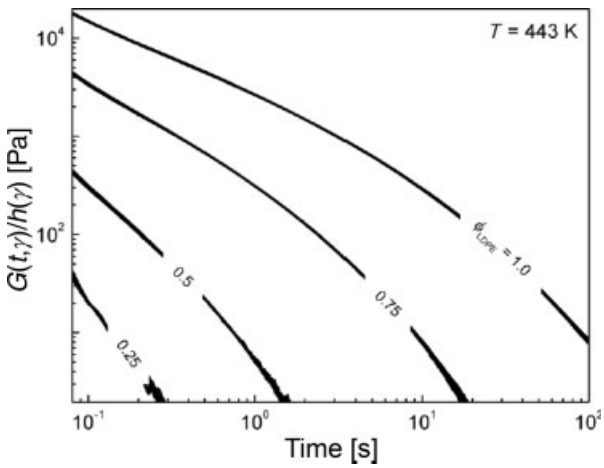

Figure 19. Reduced relaxation modulus $G(t,\gamma)/h(\gamma)$ for LDPE and LDPE/PEW blends at T = 170 °C.

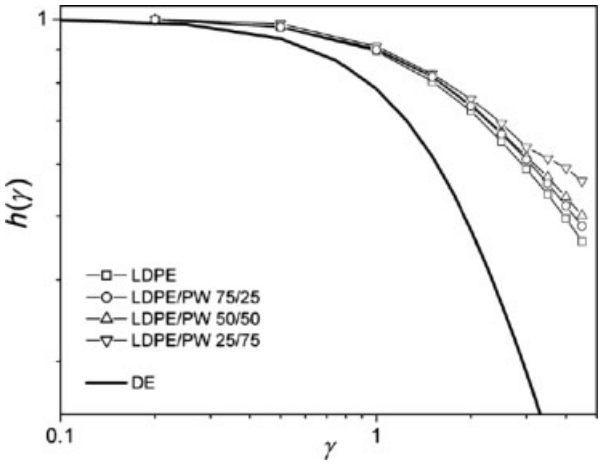

Figure 20. Damping function $h(\gamma)$ for LDPE and LDPE/linear blends at $T = 170$ °C. The solid curve is the DE damping function.

trend to what one would expect based on the BM result (eq 3).

Taken together with our results on the comb/linear/wax blends, the results on damping functions in diluted LDPE suggest a simple view of stress relaxation in LDPE. Since the molecular weight distribution is very broad, LDPE contains a relatively large amount of unentangled branched molecules (analogous to the PEW in our blends). In addition, the high molecular weight molecules in LDPE have a lot of unentangled or partially entangled branches (analogous to the relatively short arms of our comb polymers). Both of these components of LDPE will relax completely on timescales short compared to the "instantaneous" step strain in a mechanical rheometer.

The slowly relaxing portion of LDPE is then a relatively small fraction of long "backbones" of high molecular weight molecules, from which more quickly relaxing dangling arms have been "pruned". Except for extremely high molecular weight components of LDPE, these backbones will tend to be linear or three-arm stars. Only these backbone portions will support stress at late times. Because polyethylene is a very fast-relaxing molecule (low friction constant, and glass transition temperature far below crystallization), "late times" in fact means essentially all of the experimentally accessible time window with mechanical rheometry.

Figure 21 presents a cartoon of the stress-bearing portions of an LDPE melt at very early (A) and experimentally accessible "late" (B) times. At sufficiently early times, the whole set of molecules contributes to the stress. Very quickly, large portions of the melt (unentangled short molecules, and short branches) are completely relaxed, and act as a diluent. What remains is a weakly entangled or dilute solution of "backbones", which are predominantly linear or singly branched. These relax locally by Rouse dynamics (and reptation, if entangled), but much slowed down by the friction created by the decoration of short branches along the backbones.

From the molecular weight distribution for our LDPE (Fig. 18), we see that about half of the molecules (everything to the left of the peak in the distribution) have a molecular weight less than 6×10^4 g/mol. We can find an upper bound for the relaxation time of any branched structure with a given molecular weight, as follows. Because of the exponential dependence of arm retraction on arm length, at fixed total molecular weight the three-arm star is the slowest-relaxing branched structure. Bartels et al.[36] have determined the terminal relaxation time of a symmetric three arm hydrogenated polybutadiene stars with this molecular weight ($M_{arm} = 2 \times 10^4$ g/mol) at $T = 170$ °C to be about 0.01 s. Hence, half of the chains in our LDPE relax in less than 0.01 s, and play a role similar to the PEW in our comb blends.

Although LDPE is certainly not a simple, uniform, well-characterized branched model polymer, some things are known about the array of structures found in an LDPE melt. By combined used of gel permeation chromatography, dilute-solution viscometry, and light scattering, it is possible to characterize the molecular weight as well as various measures of the size of a polymer coil in dilute solution.

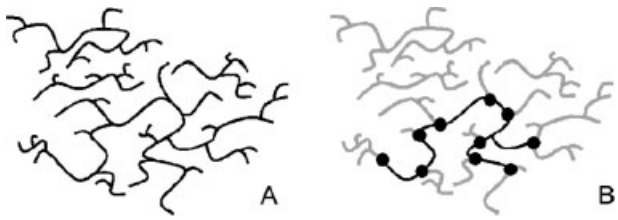

Figure 21. Cartoon of stress-bearing parts of LDPE. (A) $t = 0+$, all chains contribute to the stress tensor. (B) Quickly thereafter, low molecular weight molecules and branches are relaxed, and the stress is supported by a few long "skeletons" with friction enhanced by the presence of sidebranches.

Because branched molecules are more compact than linear chain of the same molecular weight, it is possible to infer the frequency of branches under some assumptions as to the randomness of the branched architecture. Applying such techniques gives estimates of the molecular distance between branch points, or length of dangling arms, in various LDPEs to be in the range 2000–10,000 g/mol.[37,38]

It is therefore reasonable to suppose based on the timescales we have estimated that the BM assumptions are not valid for commercial LDPE, insofar as a preponderance of the "long" branches in LDPE have a molecular weight of only a few thousand g/mol, and so relax too quickly on the experimental timescale for BM to be valid. Thus it appears from our experimental results for LDPE that the BM model is not a good description of step-strain relaxation in that system either, and for the same reason as for our model comb–linear–wax blends; namely, that the dangling arms relax too fast to contribute to the stress.

This result appears to be in contradiction with the recent findings[6,23,39] on step strain experiments for model branched polymers. Archer and Varshney[23] and Islam et al.[39] have studied the behavior of polybutadiene pom-pom polymers with three and four arms, and McLeish et al.[6] have made similar studies of polyisoprene H shaped polymers. The arm molecular weights in the three references are similar ($M_{arm} \leq 2.1 \times 10^4$ g/mol).

These authors find that $h(\gamma)$ presents an abrupt transition at values of strain similar to that expected from theory for H and pom-pom polymers. It may be that their data are contaminated with slip effects, as this work predates the paper dealing with wall slip.[17] In our case, with similar experimental conditions (cone and plate stainless steel fixtures and relatively high value of elastic modulus $G'(\omega = 100$ rad/s) greater than about 2×10^5 Pa, we found wall slip at relatively low strains in highly entangled H melts synthesized by Hadjichristidis.

In addition, the arm relaxation time for these polymers can be estimated to be lower than ~ 0.3 s for both the polybutadiene pom-poms and the polyisoprene H-polymers (see McLeish et al.[6] for details about how to estimate the terminal relaxation time of the arms in the presence of unrelaxed backbones). Then, the longest Rouse time for these arms is clearly much less than 0.3 s.

In fact, the Rouse time of the arms can be estimated as $\tau_R \sim \tau_e n_e^2$. Considering $M_{arm} = 2 \times 10^4$ g/mol the number of entanglements per arm is $n_e \sim 4$ for polyisoprene and $n_e \sim 13$ for polybutadiene. At $T = 300$ °C for polyisoprene we have $\tau_e \sim 8 \times 10^{-6}$ s and for polybutadiene $\tau_e \sim 2 \times 10^{-7}$ s. From this results that $\tau_R < 2 \times 10^{-4}$ s ($\tau_R < 4 \times 10^{-5}$ s) for polyisoprene (polybutadiene).

Thus the conditions for the validity of the Bick-McLeish model were not satisfied in these experiments, insofar as the time to impose the step of strain was larger than the Rouse time of the arms. This supports the idea that wall slip effects were responsible for the abrupt change in the behavior of $h(\gamma)$.

In fact, it is rather difficult to obtain a Rouse time of the arms larger than τ_{step} and thus to satisfy the conditions of the Bick-McLeish model in either of these polymer systems at $T = 300$ °C, because both polymers relax rather quickly. For example, to have $\tau_R \sim \tau_{step} \sim 0.1$ s with polyisoprene at $T = 300$ °C the arm molecular weight must be approximately $M_{arm} = 5.3 \times 10^5$ g/mol, resulting in impossibly slow dynamics for the total molecule.

Time-Strain Superposition for LDPE

The remarkably good time-strain superposition in a wide range of times showed in Figure 19 for LD 113 is typical of previous results for LDPE. In contrast, even linear entangled polymers show poor superposition at short times. This poor superposition at short times is also found for different model polymers, such as stars, Hs,[6] combs or pom-poms.[23]

It has been argued that the good time-strain factorability of LDPE is a result of the broad spectrum of relaxation times in such materials, which smears the non-factorability observed in model systems over a broad time window.[5]

In addition, there is another effect that improves TSS at short times in LCB polymers. According to the BKZ approach considering the effect of non-zero rise time, the failure of TSS at short times is a consequence of the contribution $Z(\gamma_0)\mathrm{d} \ln G(t)/\mathrm{d}t$ to $h(\gamma_0)$ in eq 9. As is clear from eq 13 (and the discussion immediately following), the ratio of $Z(\gamma_0)$ to $h(\gamma_0)$ is larger by a factor of about 2 ln γ_0 for damping functions like DE, compared to roughly constant damping functions.

Figure 22 shows $G(t,\gamma)$ for LDPE at two different strains ($\gamma = 0.2$ and $\gamma = 4.0$) and the results

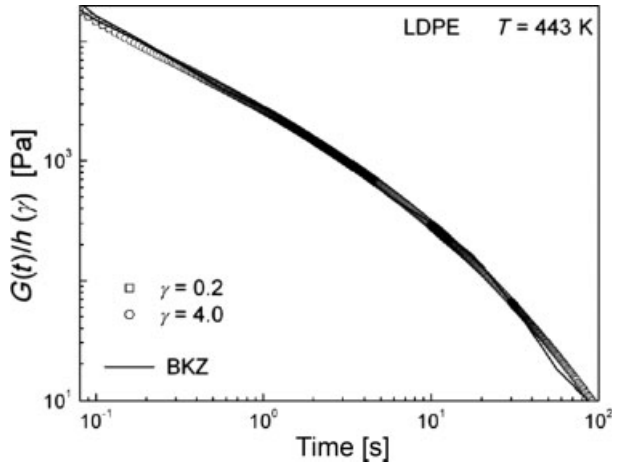

Figure 22. Reduced relaxation modulus $G(t,\gamma)/h(\gamma)$ for LDPE at two different values of strain [$\gamma = 0.2$ (squares) and $\gamma = 4.0$ (circles)]. Lines correspond to the prediction of eq 4.

of eq 4. To determine $G(t,\gamma)$ we employed the same procedure as for linear PS. Observe the good agreement between experiments and eq 4 and the reduced splitting of the curves at small times (compared to Fig. 5 for the linear chain samples).

Evidently, the BKZ model (eq 4) captures the essence of the broad applicability of TSS in our LDPE samples, relative to the linear PS. Both the shape of d ln $G(t)$/dt and the weak damping function play a role. For LDPE, with its broad smooth range of timescales, d ln $G(t)$/dt is spread out over a broad range of timescales (and is thus rather small in any particular time window). This is essentially a restatement of the McLeish-Larson argument, captured by the BKZ model.

CONCLUSIONS

We have studied the nonlinear behavior of blends containing various model and commercial branched polymer architectures through step-strain experiments. We find that upon diluting both model combs and commercial LDPE, the damping function becomes more weakly dependent on strain.

This is at odds with the qualitative behavior of the Bick-McLeish (BM) model for the damping function of entangled branched polymers. The BM model relates departures from the DE damping function, which successfully describes well-entangled linear chains, to the presence of chain segments between branch points. These segments cannot retract in the same way as segments with a dangling end, and thus bear additional stress.

The observed behavior of the damping function of our combs and LDPE samples on dilution is very similar to that observed for entangled linear chains, which when diluted show a damping function that is more nearly constant than predicted by DE. Insofar as the limit of marginally entangled chains may be described by an approach to the Rouse model, which has a constant damping function, we may expect weakly entangled linear chains to show a damping function intermediate between DE and Rouse behavior.

The observed behavior of our model comb blends can be understood in terms of "dynamic dilution". For our combs, and for commercial LDPE, the relaxation time of the dangling arms in the sample is very fast, faster even than the time a mechanical rheometer takes to make a step-strain. Thus a substantial fraction of the sample has relaxed its stress and acts like a diluent on experimental timescales.

For the model combs, the remaining stress is borne by the comb backbones, which relax very slowly because of the large friction generated by the presence of the entangled arms. The comb backbones in our samples are analogous to a slowly relaxing solution of moderately to weakly entangled linear chains. Thus it is reasonable that we find the same trend of a more constant damping function upon dilution, as is found for linear chain melts and solutions.

The BM model should not be expected to apply to such a system, since it assumes that the branched species have not yet relaxed their stress on the timescale of the step strain. For our polyethylene combs with arms of a few thousand g/mol, we estimate the relaxation timescale for the arms to be a few milliseconds, shorter than the rise time of the step strain. Of course, for branched polymers with sufficiently long and slowly-relaxing arms, the BM model should be applicable.

Remarkably, we find behavior similar to that of the model comb blends for the damping function upon diluting commercial LDPE, also at odds with expectations from the BM model. This suggests that dynamic dilution is also effective in "pruning" the LDPE chains down to a weakly entangled solution of effectively linear or weakly branched chains.

Indeed, the lengths of dangling arms and segments between branch points in LDPE (based on combining molecular weight and size information about LDPE chains in dilute solution) are estimated to be in the range of 2000–10,000 g/mol. Such dangling arms are of similar size to our comb arms, and would relax quickly on the timescale of the step-strain. This suggests that the branches in LDPE are typically too short and quickly relaxing for LDPE to be well described by the BM model.

In the course of this work we "rediscovered" two potential sources of artifacts in damping function experiments, that bear emphasizing.

Our results, as well as previous results on linear polymers from Sanchez-Reyes and Archer,[17] suggest that previous literature results concerning well- entangled polymeric systems with large elastic moduli may be contaminated by wall slip effects, irrespective of the polymer architecture. The effect of wall slip can be mitigated by dilution, or by treatment of the surface of the rheometer plates to improve the adhesion with the polymer.

As well, a relatively simple analysis using the BKZ model suggest that the non-zero rise time involved during the imposition of the step strain can contribute spuriously to the failure of time strain superposition (TSS) at short times, which was implicit in the work of Laun.[13]

As a consequence, the onset of good TSS is governed by the stress relaxation function itself, can extend many times the rise time of the step strain, and is certainly not limited by the longest Rouse time. This analysis also implies that those systems with a damping function with a relatively weak strain dependence should show better time-strain superposition at short times. In general, the effect of finite rise time in step-strain experiments has often been neglected since Laun's original work; however, we find it to be an important consideration in analyzing step-strain data.

Examining well entangled star/linear blends, we find some unexpected and puzzling characteristics, such as a damping function with a stronger dependence on strain than DE at intermediate times. The expected result, that star melts and solutions should have a damping function described by DE (because the dangling end of each arm permits retraction just as for linears), is not well satisfied. The reason for this is not clear.

Finally, we note that at present there is no detailed theory describing the damping function one should expect for weakly entangled effectively linear chains, which this work suggests is an important class of systems to which both diluted combs and LDPE belong.

We thank Nikos Hadjichristidis and David J. Lohse for supplying the model polyethylenes used in this study, and Bill Graessley for many useful conversations and much encouragement. DAV express his gratitude to Fundación Antorchas and the National Research Council of Argentina (CONICET) for financial support.

REFERENCES AND NOTES

1. Doi, M.; Edwards, S. F. The Theory of Polymer Dynamics; Clarendon: Oxford, 1986.
2. Milner, S. T.; McLeish, T. C. B. Macromolecules 1997, 30, 2159.
3. Milner, S. T.; McLeish, T. C. B. Phys Rev Lett 1998, 81, 725.
4. Milner, S. T.; McLeish, T. C. B.; Young, R. N.; Hakiki, A.; Johnson, J. M. Macromolecules 1998, 31, 9345.
5. McLeish, T. C. B.; Larson, R. G. J Rheol 1998, 42, 81.
6. McLeish, T. C. B.; Allgaier, J.; Bick, D. K.; Bishko, G.; Biswas, P.; Blackwell, R.; Blottiere, B.; Clarke, N.; Gibbs, B.; Groves, D. J.; Hakiki, A.; Heenan, R. K.; Johnson, J. M.; Kant, R.; Read, D. J.; Young, R. N. Macromolecules 1999, 32, 6734.
7. Daniels, D. R.; McLeish, T. C. B.; Crosby, B. J.; Young, R. N.; Fernyhough, C. M. Macromolecules 2001, 34, 7025.
8. Osaki, K.; Nishizawa, K.; Kurata, M. Macromolecules 1982, 15, 1068.
9. Vrentas, C. M.; Graessley, W. W. J Rheol 1982, 26, 359.
10. Soskey, P. R.; Winter, H. H. J Rheol 1985, 29, 493.
11. Samurkas, T.; Larson, R. G.; Dealy, J. M. J Rheol 1989, 33, 559.
12. Fukuda, M.; Osaki, K.; Kurata, M. J Polym Sci Part B: Polym Phys 1975, 13, 1563.
13. Laun, H. M. Rheol Acta 1978, 17, 1.
14. Osaki, K.; Kurata, M. Macromolecules 1980, 13, 671.
15. Wagner, M. H. Rheol Acta 1976, 15, 135.
16. Osaki, K. Rheol Acta 1993, 32, 429.
17. Sanchez-Reyes, J.; Archer, L. A. Macromolecules 2002, 35, 5194.
18. Inoue, T.; Uematsu, T.; Yamashita, Y.; Osaki, K. Macromolecules 2002, 35, 4718.
19. Soskey, P. R.; Winter, H. H. J Rheol 1984, 28, 625.
20. Bick, D. K.; McLeish, T. C. B. Phys Rev Lett 1996, 76, 2587.

21. Bishko, G.; McLeish, T. C. B.; Harlen, O. G.; Larson, R. G. Phys Rev Lett 1997, 79, 2352.
22. Inkson, N. J.; McLeish, T. C. B.; Harlen, O. G.; Groves, D. J. J Rheol 1999, 43, 873.
23. Archer, L. A.; Varshney, S. K. Macromolecules 1998, 31, 6348.
24. Kasehagen, L. J.; Macosko, C. W. J Rheol 1998, 42, 1303.
25. Gevgilili, H.; Kaylon, D. M. J Rheol 2001, 45, 467.
26. Bernstein, B.; Kearsley, E. A.; Zapas, L. J. Trans Soc Rheol 1963, 7, 391.
27. Hadjichristidis, N.; Xenidou, M.; Iatrou, H.; Pitsikalis, M.; Poulos, Y.; Avgeropoulos, A.; Sioula, S.; Paraskeva, S.; Velis, G.; Lohse, D. J.; Schulz, D. N.; Fetters, L. J.; Wright, P. J.; Mendelson, R. A.; Garcia–Franco, C. A.; Sun, T.; Ruff, C. J. Macromolecules 2000, 33, 2424.
28. Colby, R.; Rubinstein, M. Macromolecules 1990, 23, 2753.
29. Fetters, L. J.; Lohse, D. J.; Richter, D.; Witten, T. A.; Zirkel, A. Macromolecules 1994, 27, 4639.
30. Watanabe, H.; Matsumiya, Y.; Osaki, K. J Polym Sci Part B: Polym Phys 2000, 38, 1024.
31. Osaki, K.; Takatori, E.; Kurata, M.; Watanabe, H.; Yoshida, H.; Kotaka, T. Macro-molecules 1990, 23, 4392.
32. Pearson, D. S.; Fetters, L. J.; Strate, G. V.; von Meerwall, E. Macromolecules 1994, 27, 711.
33. Graessley, W. W.; Raju, V. R. J Polym Sci Polym Symp 1984, 71, 77.
34. Likhtman, A. E.; Milner, S. T.; McLeish, T. C. B. Phys Rev Lett 2000, 85, 4550.
35. Crosby, B. J.; Mangnus, M.; de Groot, W.; Daniels, R.; McLeish, T. C. B. J Rheol 2002, 46, 401.
36. Bartels, C. R.; B. C. Jr., Fetters, L. J.; Graessley, W. W. Macromolecules 1986, 19, 785.
37. Mendelson, R. A.; Bowles, W. A.; Finger, F. L. J Polym Sci Part A-1: Polym chem 1970, 8, 105.
38. Wild, L.; Ranganath, R.; Ryle, T. J Poly Sci Part A-1: Polym chem 1971, 9, 2137.
39. Islam, M.; Juliani, T.; Archer, L. A. Macromolecules 2001, 34, 6438.